National Aeronautics and Space Administration

Digest on Performance of COTS EEE Parts Under Extreme Temperatures

NASA Electronic Parts and Packaging (NEPP) Program
Office of Safety and Mission Assurance

Kristen Boomer
NASA Glenn Research Center
Cleveland, Ohio

Ahmad Hammoud
HX5, LLC
Cleveland, Ohio

Digest on Performance of COTS EEE Parts Under Extreme Temperatures

Scope

The NASA Glenn Research Center has been performing reliability studies and performance evaluation of commercial-off-the-shelf (COTS) Electrical, Electronic, and Electromechanical (EEE) parts in the typical harsh space environment, in particular extreme temperature exposure and wide-range thermal cycling. These efforts have spanned several years under the support of the NASA Electronic Parts and Packaging (NEPP) Program. Sometimes, the performance assessments of NASA-developed parts and materials were also executed in collaboration with other NASA Centers including GSFC, LaRC, MSFC, and JPL. Test articles comprised semiconductor switches, capacitors, oscillators, voltage references, flexible printed circuit boards, sensors, and DC/DC converters, to name a few. While this digest provides a synopsis on test results obtained on selected parts, detailed findings specific to these and other COTS parts are posted on the NASA NEPP website. The experimental investigations, which focused mainly on exposure of the devices/circuits to both high and low temperatures (occasionally beyond their specified limits), thermal cycling, and re-start capability at temperature extremes, were carried out to establish a baseline on the functionality and to determine suitability of these devices for use in space exploration missions. The findings are disseminated to mission planners and circuit designers so that proper selection of electronic parts can be made, and risk assessment and mitigation techniques are established to use such devices in space missions.

Extreme Temperature Environment

Electronic circuits and systems for future NASA space missions involve spacecraft, deep space probes, planetary orbiters and landers, and surface exploratory instrumentation that require reliable and efficient operation in extreme temperature environments. For example, an interplanetary probe launched to explore the rings of Saturn would experience a temperature of about -138 °C. The average temperature of planetary solar system is shown in Table I [1]. Commercial-grade electronic parts are typically specified to operate between 0°C and 70°C, industrial-grade semiconductor devices are specified to operate between -40°C and 85°C, and military-grade ones are specified to operate between -55°C and 125°C. The ratings of parts intended for space use are different due to the stringent temperature envelope and, therefore, require operation well outside the range of available EEE Parts.

Table I. Average Temperature of Planetary Solar System [1]

Planet	Average Temperature (°C)
Venus	471
Mercury	430
Mars	-28
Jupiter	-108
Saturn	-138
Uranus	-195
Neptune	-201

Presently, spacecraft operating in cold-temperature regions must utilize some kind of heating mechanism in order to maintain an operating temperature for the on-board electronics of approximately 20 °C. The conventional heating elements used require associated containment structures and thermal systems such as shutters to maintain the 20 °C temperature over the course of the entire mission. However, if the electronics were capable of operating at the temperature of the mission environment, these heating units and their associated structures and thermal systems could be eliminated, reducing system size and weight, improving reliability, and extending lifetime. Similarly, operating electronics in high temperature environments necessitates the removal of internally-generated heat, especially for power-level devices, to provide efficient operation and to prevent thermal runaway, which can ultimately cause severe device degradation, if not catastrophic failure. Removal of the excess heat is usually accomplished via the use of radiators, passive or active heat pipes, or other mechanisms that again will result in overall system design complexity, increased weight and size, and impacting reliability. Thus, it becomes apparent that extreme temperature electronics would remove the need for thermal control elements and their associated structures for proper ambient operation. Besides decreased system mass and size, simplified design complexity, and reduced power requirements, other advantages are realized in the form of shortened development time and effort, reduced launch costs, as well as extended mission operations for longer observation and exploration.

Other benefits are gained as well through the availability of extreme temperature operation. For example, better electronic, electrical, and thermal properties of certain materials are attained at low temperatures [2]-[3]. In particular, the performance of certain semiconductor devices improves with decreasing temperature down to liquid nitrogen temperature (–196 °C). At low temperatures, majority carrier devices demonstrate reduced leakage current and reduced latch-up susceptibility [3]-[4]. In addition, these devices show higher speed resulting from increased carrier mobility and saturation velocity [3]-[5]. An example is the power Metal-Oxide-Semiconductor Field-Effect Transistor (MOSFET), which has lower conduction losses at low temperature due to the reduction in the drain-to-source resistance RDS(on) resulting from increased carrier mobility [4], [6]-[7]. At the other end of temperature spectrum, electronic parts based on silicon-on-insulator (SOI) technology provide faster switching, consume less power, and offer better radiation-tolerance compared to their conventional counterparts. They also exhibit reduced current leakage and, thus, they are often tailored for high temperature operation. Similar traits can be attributed to the new emerging wide bandgap semiconductor technologies, namely silicon carbide and gallium nitride, especially in the power electronics area.

In addition to deep space applications, electronics that can operate under extreme low temperatures have potential uses in terrestrial applications that include magnetic levitation transportation systems, medical diagnostics, cryogenic instrumentation, and super-conducting magnetic energy storage systems. Aircraft engines, power generation facilities, automotive, down-hole instruments, and all-electric boats and aircraft, on the other hand, require high temperature electronics.

Power MOSFETs

The gate threshold voltage (V_{TH}) and drain-to-source on-state resistance ($R_{DS(on)}$) of an SOI and silicon (Si) power MOSFETs are shown in Figures 1 and 2, respectively. The Honeywell HTANFET is a high temperature N-channel power FET fabricated using SOI processes, while the Si device tested was an International Rectifier IRFD110 HEXFET Power MOSFET. As seen in Figure 1, both devices exhibit an increase in gate threshold voltage with decreasing temperature. The Si MOSFET, which has a maximum specified gate voltage of 20V, exhibits a gate threshold voltage in the range of 3.03V to 3.92V from 20 °C to -190 °C. This corresponds to a normalized gate threshold voltage (V_{TH})/V_{GS} (max) between 0.152 and 0.196. The SOI MOSFET, which has a maximum specified gate voltage of 10V, displays a gate threshold voltage in the range of 1.64V to 2.21V from 20 °C to -190 °C. This corresponds to a normalized gate

threshold voltage range of 0.164 to 0.221. In general, both devices show comparable changes in gate threshold voltage with change in temperature.

Figure 2 shows the drain-to-source on-state resistance ($R_{DS(on)}$) versus temperature for the two devices. On-state resistance values were obtained at a drain current of 0.6A and a gate voltage of 8V for the Si MOSFET, and at a drain current of 0.6A and a gate voltage of 5V for the SOI MOSFET. As can be seen from Figure 2, both devices exhibit a decrease in on-state resistance with decreasing temperature down to - 175 °C. Beyond this temperature, the on-state resistance for both devices, however, begins to increase as temperature is decreased further. At any given temperature, the SOI has a slightly higher on-state resistance than the Si MOSFET.

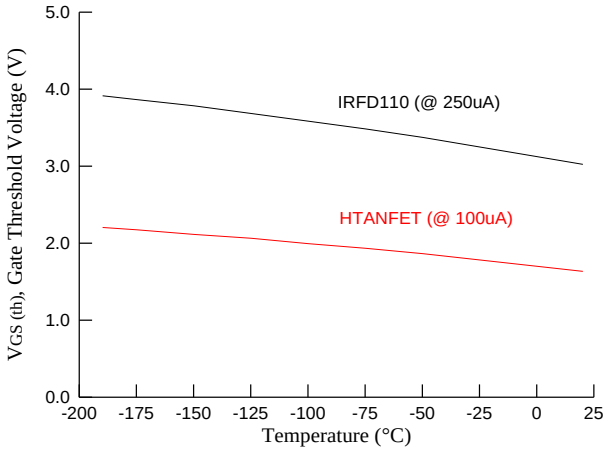

Figure 1. Gate threshold voltage for SOI and Si MOSFETs vs. temperature

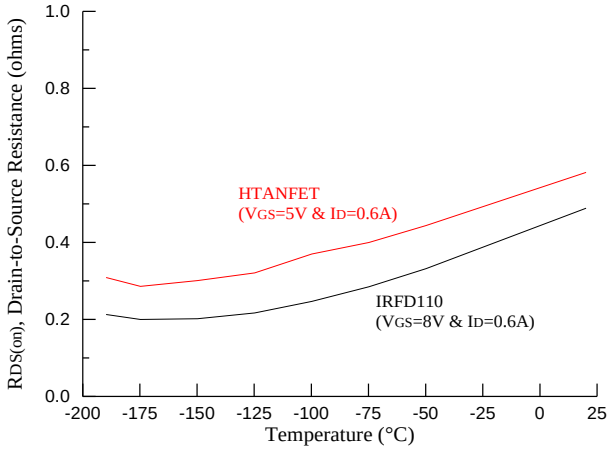

Figure 2. Drain-to-source resistance for SOI and Si MOSFETs vs. temperature

MOSFET SOI-Driver

The characteristics of an SOI bridge driver with an internal adjustable oscillator, designed for driving MOSFETs in a full bridge configuration as depicted in Figure 3, were obtained under wide temperature range between -195 °C and +85 °C and thermal cycling. Waveforms of the driver output signals gate higher right output MOSFET (GHR), gate lower right (GLR) output MOSFET, gate higher left (GHL) output MOSFET, and gate lower left (GLL) output MOSFET obtained at 20, -195, and +85 °C are shown in Figure 4. No major change or distortion was observed in the shape or magnitude of these waveforms throughout the test temperature range, and cold-start capability was successful. Thermal cycling of the driver integrated circuit (IC) chip had no effect as the post-cycling modulated outputs at any given test temperature were the same as those obtained prior to cycling, as shown for pre- and post-cycling conditions at the test temperatures of +20, -195, and +85 °C in Figure 5. The thermal cycling also appeared to have no effect on the structural integrity of this device as no structural deterioration or packaging damage was observed.

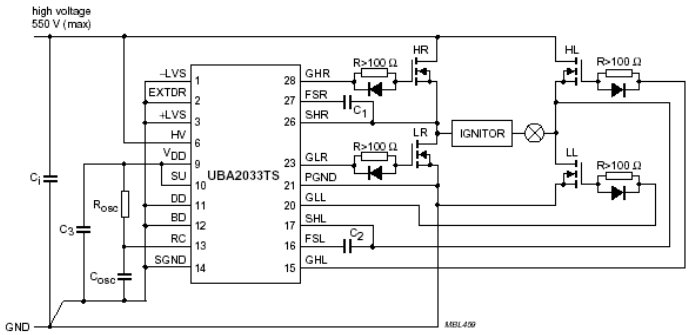

Figure 3. Schematic of circuit used in the evaluation of full bridge driver SOI IC chip.

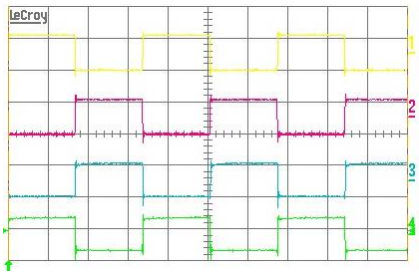

at +20°C

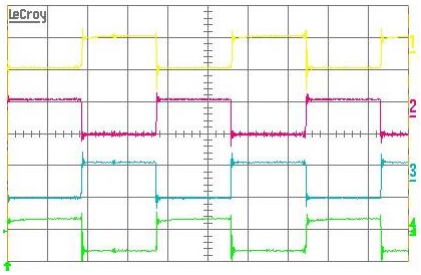

at -195°C

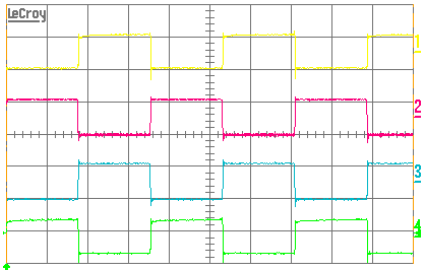

at +85°C

Figure 4. Waveforms of driver output signals GHR (1), GLR (2), GHL (3), and GLL (4) at various temperatures.

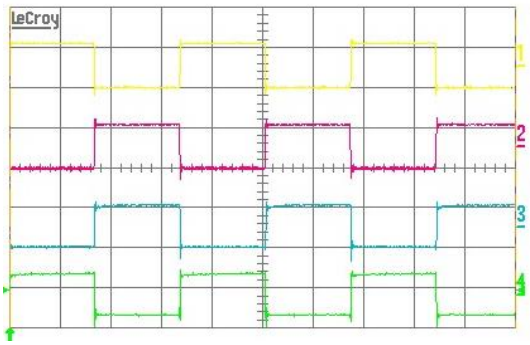

Pre-cycling at +20 °C

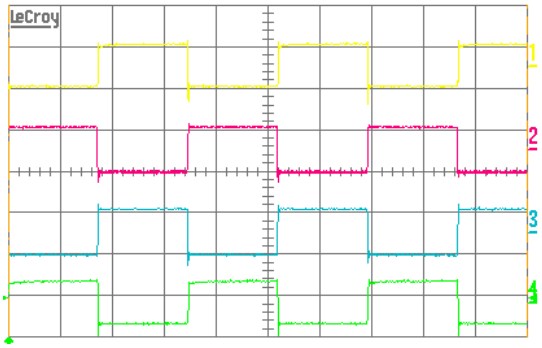

Post-cycling at +20 °C

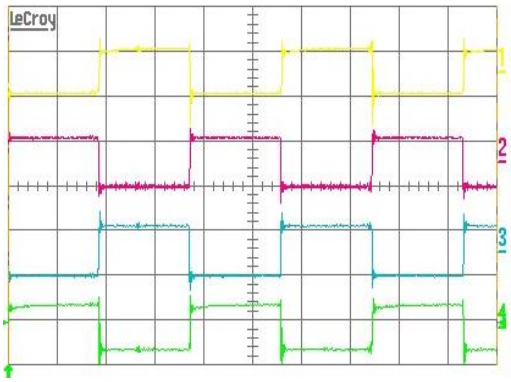

Pre-cycling at -195 °C

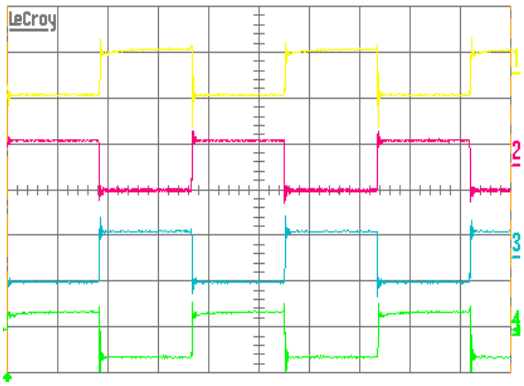

Post-cycling at -195 °C

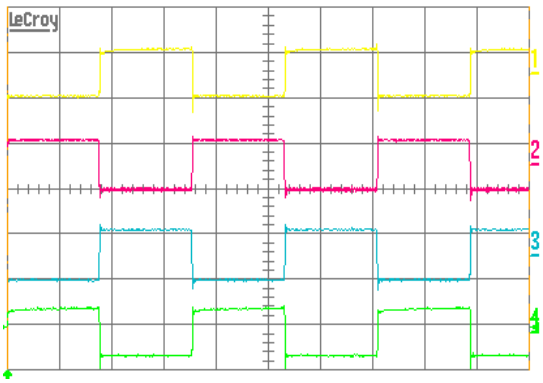

Pre-cycling at +85 °C

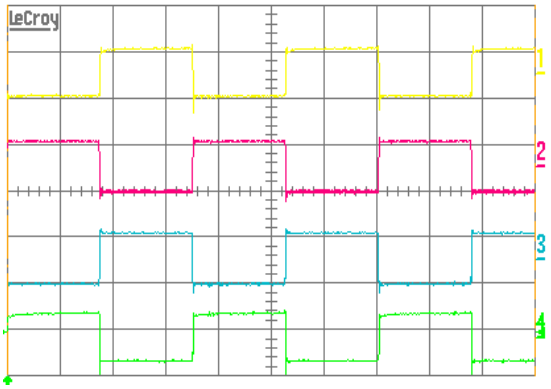

Post-cycling at +85 °C.

Figure 5. Pre- & post-cycle waveforms of SOI driver outputs GHR, GLR, GHL, and GLL at various temperatures.

SOI Monolithic Quad Operational Amplifier

A monolithic quad operational amplifier using silicon-on-insulator technology process and designed for use in high temperature environments was evaluated under extreme temperatures. The ceramic-packaged chip is specified for -55 °C to +225 °C operation with a 15 mA output current capability, and it can operate from a single or dual supply. An amplifier circuit configured in a unity gain, inverting configuration was constructed utilizing the SOI chip and a few passive components. The circuit was evaluated in the temperature range between -195 °C to +200 °C in terms of signal gain, phase shift, and supply current. These properties were recorded at selected test temperatures in the frequency range of 1 kHz to 10 MHz. In addition, the circuit was exposed to a total of 10 cycles between -195 °C and +200 °C at a temperature rate of 10 °C/minute. Following the thermal cycling, circuit measurements were then performed at the test temperatures of +25, -195, and +200°C.

The gain and phase shift of the amplifier at various test temperatures in the frequency range of 1 kHz to 10 MHz is shown in Figure 6. It can be clearly seen that the gain of the amplifier remained relatively the same, regardless of the test temperature, until the test frequency of about 400 kHz was reached. Beyond that frequency, gain rolled off as a function of temperature. However, this dependency was slight and it seemed to occur most notably at the extreme cryogenic temperature, i.e. -150 and -195 °C. In the high temperature regime, the amplifier's gain did not exhibit much deviation from its room temperature characteristics. While the roll-off frequency (-3 dB gain) at room temperature was at 850 kHz, it slightly increased to about 1 MHz at +200 °C, and dropped to about 500 kHz at -195 °C. As far as the frequency is concerned, the gain began to show appreciable drop above 4 MHz. This drop in the gain at very high frequencies is typical of most operational amplifiers. The data depicted in Figure 6, thus, indicate that the amplifier circuit had operated well in the temperature range between -195 °C and +200 °C. Similar to the gain characteristics, the phase exhibited very slight changes only at the extreme cryogenic temperatures and at frequencies above 400 kHz.

The amplifier's gain and phase obtained after thermal cycling is shown in Figure 7 as a function of frequency at the selected test temperatures of +200, +25, and -195 °C. It can be clearly seen that these results were very similar to those obtained prior to cycling that are depicted in Figure 6 and, thus, it can be concluded that the thermal cycling had no effect on the amplifier's gain or phase margin. In addition to

maintaining its electrical performance with cycling, the operational amplifier chip did not suffer any deterioration or damage in its packaging due to this limited thermal cycling.

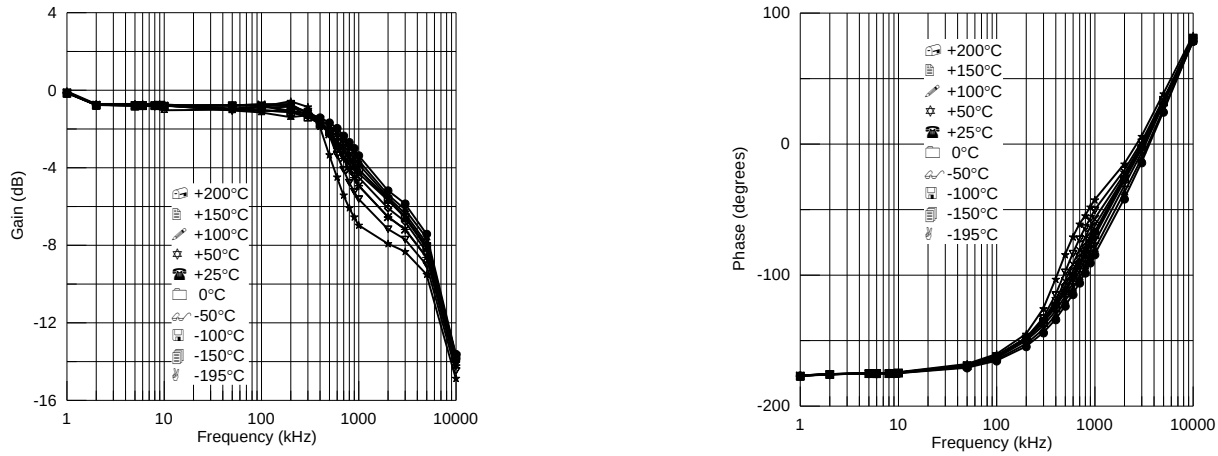

Figure 6. Gain & phase versus frequency at various temperatures prior to thermal cycling.

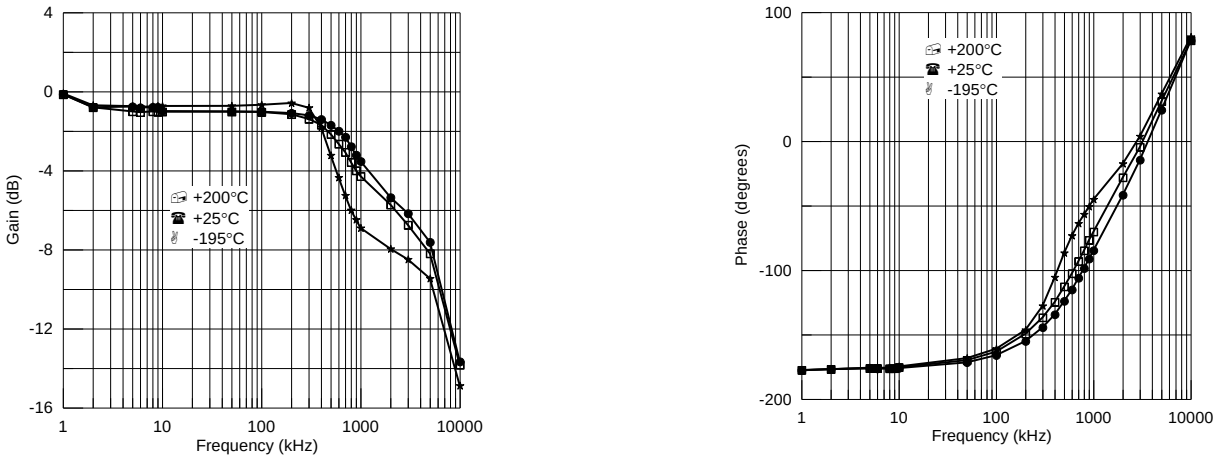

Figure 7. Gain & phase versus frequency at various temperatures after thermal cycling.

DC/DC Converters

The performance of nine low-to-medium power COTS modular DC/DC converters was evaluated under cryogenic temperatures in terms of their output regulation, efficiency, and input and output current characteristics. At a given temperature, these properties were obtained at various input voltages and at different load levels; from no-load to full-load conditions. The tests were performed as a function of temperature using an environmental chamber cooled by liquid nitrogen using a temperature rate of change of 10 ºC/min. Each of the test articles were allowed to soak for a period of 30 minutes at the selected test temperature so that thermal stability was achieved prior to recording measurements. Table II lists some of the specifications of these DC/DC converters.

Table II. DC/DC Converter Module Specifications and Performance

Converter Specifications					
Manufacturer	**Part Number**	**Input Voltage (V)**	**Output Voltage (V)**	**Rated Power (W)**	**Operating Temperature (°C)**
Astrodyne	ASD10-12S3	9 - 36	3.3	10	-40 to 60
Power Trend	PT4110A	36 - 72	3.3	10	-40 to 85
Lambda	PM10-24S03	18 - 36	3.3	10	-40 to 70
Power One	DFA20E24S3.3	18 - 36	3.3	13	-40 to 85
CDI	1003S12HN	9 - 36	3.3	10	-40 to 85
Interpoint	SMHF283R3S/KR	16 - 40	3.3	15	-55 to 125
Calex	24S3.15HE	18 - 36	3.3	75	-40 to 100
SynQor	PQ48050HNA30	36 - 75	3.3	100	-40 to 115
Vicor	V48C12C150A	36 - 75	12	150	-20 to 100

The results obtained on the evaluations of the nine DC/DC converters varied widely in terms of extending capability of operation at temperatures lower than their specified limit. A brief summary on the performance of each of the converters is described in Table III. It is important to note that any observed variation in the operational characteristics or the malfunctioning exhibited by any or all of the tested converters due to exposure to the cryogenic test temperatures was transitory in nature as all devices recovered upon elimination of the cold temperature stress.

Table III. Performance Summary of Tested Converters

Converter	Operating Temperature (°C)	Experimental Observations	Decisive* Temperature (°C)
Astrodyne	-40 to 60	V_{out} dropped to 2.4 V at –140 °C. Chip functioned down to –160 °C.	-160
Power Trend	-40 to 85	V_{out} lost regulation at –100 °C. Converter still functioned to –195 °C.	-195
Lambda	-40 to 70	Chip worked very well down to -120 °C. Input current oscillations occurred at all temperatures under heavy loading.	-120
Power One	-40 to 85	Oscillations in input current started at –80 °C.	-120
CDI	-40 to 85	Oscillations in input current observed at –140 °C under heavy loading.	-180
Interpoint	-55 to 125	Low frequency oscillations with high peaks observed in input current at –120 °C and below.	-160
Calex	-40 to 100	Although the module ceased to work at -40 °C during steady state, it worked down to -100 when tested under a step change in load from full to no-load and vice-versa.	-40
SynQor	-40 to 115	Output voltage increased as temperature was lowered below 20 °C.	-80
Vicor	-20 to 100	Oscillation in input current started at –40 °C; more noticeable under heavy load conditions.	-120

* Temperature at which module ceased to operate.

The results depicted in Table III indicated that while some of the DC/DC converters continued to function at low temperatures well below their specified limit, others did not fare as well. The difference in the performance of these devices could be attributed to many factors which include:

- Design topology and architecture of the converter module such as buck, boost, etc.
- Selection of material used in the manufacturing of the modules, as electrical, chemical, and physical properties are temperature-dependent. For instance, diode voltage drop, transistor threshold voltage, capacitor dielectric loss, and inductor quality factor are very much influenced with temperature variation.
- Temperature-induced offset or drift in the biasing conditions for proper operation of some of the module's on-board components.
- Sensitivity of the individual parts to combined effects of electrical (loading) and thermal stressing.

Resistors

Several types of low to medium power resistors were evaluated in terms of resistance stability as a function of temperature. These passive devices included metal film, carbon and ceramic composition, thin and thick film, wire wound, and power film resistors. Manufacturer specifications of these resistors

are listed in Table IV. Two values of each type of resistor were selected in this evaluation. These values were 10 Ω (or closest value if unavailable) and 1 kΩ. For each type of resistor, two devices of the same value were included in this work to confirm certainty and validity of the performance of the resistor under test. The resistors were evaluated in the frequency range of 10 Hz to 500 kHz using four-wire measurements at various test temperatures between +25 °C and -190 °C. Limited thermal cycling between +25 °C and -190 °C was also performed on the resistors.

Table IV. Manufacturer Specifications of Resistors

Type	Value (Ω)	Tol. (%)	Voltage (V)	PWR (W)	Temp (°C)	Temp Coeff (ppm/°C)	Package	Manufacturer	Part #
Metal Film	10	±1	250	0.5	-55 to +175	±25 to ±200	Axial	Vishay/Dale	CMF55C10
	1K	±1	250	0.5	< +170	±50	Axial	Vishay	CT551K0FT2
Wire Wound	10	±5	495	5	< +350	±30	Axial	Ohmite	95J10R
	1K	±5	495	5	< +350	±30	Axial	Ohmite	95J10K0
Thin Film	33	(±1 Ω)	200	1.6	-55 to +125	±250	Single-in-line	Bourns	4608X-102-330
	1K	±2	200	1.6	-55 to +125	±100	Single-in-line	Bourns	4608X-102-102
Thick Film	100	±2	100	0.3	-55 to +125	±100	Single-in-line	Dale	CSC08A-03-101G
	1K	±2	100	0.2	-55 to +125	±100	Single-in-line	Dale	CSC08A-01-102G
Carbon Film	10	±5	250	0.25	< +155	±350	Axial	Ohmite	OK1005
	1K	±5	250	0.25	< +155	-450	Axial	Ohmite	OK1025
Carbon Composition	15	±5	250	0.25	< +130	--	Axial	Ohmite	OD150J
	1K	±5	250	0.25	< +130	--	Axial	Ohmite	OD102J
Ceramic Composition	10	±10	500	1	< +200	-1300±300	Axial	Ohmite	OX100K
	1K	±10	500	1	< +200	-1300±300	Axial	Ohmite	OX102K
Power Film	10	±1	300	20	-55 to +175	-20 to +50	TO-220	Caddock	MP820-10.0-1
	1K	±1	300	20	-55 to +175	-20 to +50	TO-220	Caddock	MP820-1.0K-1

While some of these resistors showed excellent stability with temperature down to –190ºC, others did not fare as well, as shown in Table V. Figure 8 gives a graphical illustration of the resistor type and the corresponding change in resistance at the extreme low temperature of –190 °C.

Table V. Resistance and Percentage Change at –190 °C (@ 1 kHz)

Type	Value (Ω)	Resistance (Ω) at 25 °C	Resistance (Ω) at -190 °C	Change in Resistance (%) at -190 °C
Metal Film	10	10.00	9.99	0.0
	1K	999.15	1001.86	0.3
Wire wound	10	9.70	9.62	-0.9
	1K	984.80	979.31	-0.6
Thin Film	33	33.07	34.32	3.8
	1K	995.41	1007.88	1.3
Thick Film	100	99.99	105.42	5.4
	1K	998.70	1003.22	0.5
Carbon Film	10	9.96	10.46	5.1
	1K	980.30	1035.83	5.7
Carbon Composition	15	14.65	16.34	11.6
	1K	1013.29	1296.54	28.0
Ceramic Composition	10	9.49	10.99	15.8
	1K	993.09	1167.51	17.6
Power Film	10	10.00	10.48	4.9
	1K	996.20	1037.06	4.1

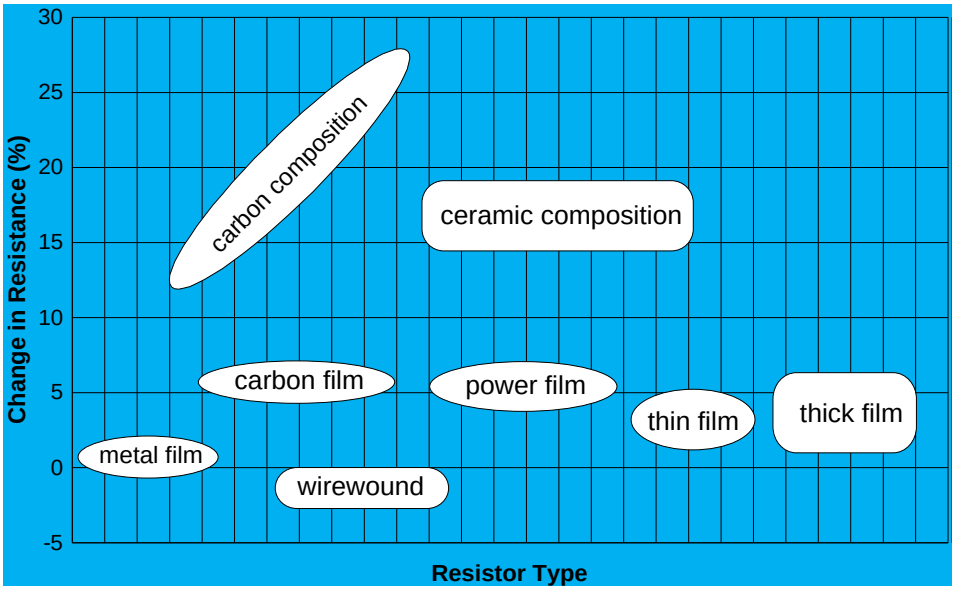

Figure 8. Percent change in resistance at –190 °C versus resistor type.

Conclusions

Representative data obtained on several COTS electronic parts were presented in this digest. This work was performed under the support of the NASA NEPP Program and addressed performance and reliability of the investigated test articles under extreme temperature exposure and wide-range thermal cycling. Detailed test results and discussions pertaining to these specific parts are posted on the NASA NEPP website. A follow-on digest covering other tested COTS parts will follow.

[1]. https://solarsystem.nasa.gov/resources/681/solar-system-temperatures/

[2]. Kirschman, R K 1991: Low temperature electronic device operation, Symposium of Electrochemical Society, 14.

[3]. Dean, M, Foty D, Saks, N, Raider, S, & Oleszel, G 1991: *Low temperature microelectronics: opportunities and challenges*, Proc. Symposium on Low Temperature Electronic Device Operation, Electrochemical Society, 91,14, 25-37.

[4]. Ray, B, Gerber, S, Patterson, R L, & Myers, I T 1995: *Power control electronics for cryogenic instrumentation*, Advances in Inst. and Control, 50, 1, Int. Soc. for Measurement and Control, 131-139.

[5]. Krishman, R K 1985: *Cold electronics: an overview*, Cryogenics, 25, 3, 115-122.

[6]. Mueller, O 1989: *On-resistance, thermal resistance and reverse recovery time of power MOSFETs at 77K*, Cryogenics, 29, 1006-1014.

[7]. Ray, B, Gerber, S, Patterson, R L, & Myers, I T 1995: *77K Operation of a multi-resonant power converter*, IEEE PESC'95 Record, 1, 55-60.

Acknowledgements

This work was performed in support of the NASA Electronic Parts and Packaging (NEPP) Program. Part of this effort was done at the NASA Glenn Research Center under GEARS Contract 80GRC020D0003.